A Novel Methodology for Generating Thermal Scattering Cross Sections and Uncertainties[1]

Chris W. Chapman,[1] Farzad Rahnema,[1] Luiz Leal,[2] Yaron Danon,[3] Goran Arbanas,[4]

[1]*Georgia Institute of Technology, North Avenue, Atlanta, GA 30332,USA*
[2]*IRSN, PSN-EXP/SNC/LNR, Fontenay-aux-Roses, France*
[3]*Rensselaer Polytechnic Institute: 110 8th Street, Troy, NY 12180, USA*
[4]*Oak Ridge National Laboratory, PO Box 2008, MS 6171, Oak Ridge, TN 37831-6171*
chapmancw@ornl.gov

INTRODUCTION

With the rise in interest of GEN-IV reactor systems, newer, and more accurate thermal scattering nuclear data are needed. Both GEN-IV reactors and current light water reactors applying for license extensions require high fidelity cross sections and uncertainties to better thermal margins and thereby maximizing energy production and improving economics and safety. Thermal moderator data play a key role in both reactor physics and nuclear criticality safety analyses. Due to the lack of uncertainties data for thermal scattering material, there is no way to quantify the effects of thermal scattering uncertainties in quantities of interest (e.g., k_{eff}) in reactor or criticality safety systems.

The framework outlined here aims to alleviate these issues by providing a generalized method to generate thermal scattering double differential cross sections (DDCSs) and their respective uncertainties from model parameters. This is accomplished by fitting the computer-simulated scattering data against experimental data using the Unified Monte Carlo (UMC) method. This method had previously only been used on fast spectrum data [1]. The UMC method is tested on light water systems, as it is of significant importance to both reactor systems as well as criticality safety. These new cross sections are then validated against experimental benchmarks and other experimentally gathered cross section data.

THEORY AND IMPLEMENTATION

To generate the light water DDCSs and their uncertainties, a simulation of 512 light water molecules were modeled in the classical molecular dynamics code GROMACS [2]. The molecules were parameterized using the TIP4P/2005f potential [3]. The simulation time was 100 ps with a timestep of 0.1 fs at constant volume and temperature. This leads to a ΔE of 0.05 meV and an E_{max} of 10 eV. These simulations computed the velocity autocorrelation function, which were then used to generate the frequency distribution. The frequency distribution are necessary to calculate the intermediate structure factor, shown in Eq. (1),

$$F(q,t) = \exp\left[-\frac{q^2}{2}\frac{\hbar}{m}\int_0^\infty d\omega \frac{\rho(\omega)}{\omega} \times \left\{ \coth\left(\frac{\hbar\omega}{2k_B T}\right)(1-\cos(\omega t)) - i\sin\omega t)\right\}\right], \quad (1)$$

where q is the momentum transfer defined as $\hbar q = \hbar|\mathbf{q_i} - \mathbf{q_f}|$, m is the mass of the scattering target, ω is the energy transfer such that $\hbar\omega = E_i - E_f$, k_B is the Boltzmann constant, T is the temperature of the scattering material, and $\rho(\omega)$ is the frequency distribution. The incoherent contribution, when there is no interference between scattering neutron wavefunctions, is represented by the incoherent approximation, as demonstrated by Abe and Tasaki [4]. The coherent contribution, which occurs when neutrons scatter with different nuclei and their wavefunctions constructively interfere with one another, is neglected here.

While other methods take the coherent contribution [5] into account, the incoherent approximation is sufficient for describing water since the incoherent scattering cross section (160.54 b) is sufficiently larger than the coherent scattering cross section (7.7486 b). From here, the dynamic structure factor $S(q,E)$ was calculated by performing a Fourier transform on the intermediate structure factor. This was done using an in-house code that performs the Fourier transform, makes the necessary transform to $S(\alpha,\beta)$, and writes it out in ENDF6 format. This structure factor was then used to generate an ACE file for use by Monte Carlo n-Particle (MCNP) [6] code using the ACER module of NJOY [7] to better model the Spallation Neutron Source (SNS) experimental setup. Finally, the SNS resolution function, a function that was provided to us by the SNS experimentalists [8] and is dependent on the energy transfer E, was applied to these results.

This process was repeated several thousand times. Each time, the individual parameters of the TIP4P/2005f potential were changed slightly. Each parameter was randomly sampled from a Gaussian distribution with a variance of 5% (the exact value varied from parameter to parameter). There is no justification for why 5% specifically was chosen as opposed to another value. There were many runs that would fail because the randomly chosen parameters lead to nonphysical results. These ensembles were rejected; ultimately, 3,000 ensembles that were able to run to completion. Of these 3,000 ensembles, only 60 met the more stringent criteria of being within 5% of the experimental diffusion coefficient. Other properties of water (density, relative static dielectric constant, isothermal compressibility, and dipole moment), agreed very favorably with their experimental values, but this was expected with

[1]This manuscript has been authored by UT-Battelle, LLC under Contract No. DE-AC05-00OR22725 with the U.S. Department of Energy. The United States Government retains and the publisher, by accepting the article for publication, acknowledges that the United States Government retains a non-exclusive, paid-up, irrevocable, world-wide license to publish or reproduce the published form of this manuscript, or allow others to do so, for United States Government purposes. The Department of Energy will provide public access to these results of federally sponsored research in accordance with the DOE Public Access Plan (http://energy.gov/downloads/doe-public-access-plan).

the strict restrictions on diffusion coefficient. Limiting the ensembles by the diffusion coefficient ensured that the density of states were the most accurate since the diffusion coefficient can be directly calculated from the density of states. Once these runs were finished, the ensembles of DDCSs were used to calculate the weighting functions from the UMC-B method shown in Eq. 2

$$\omega_k = \exp\left\{-\frac{1}{2}\left[(\mathbf{y}_k - \mathbf{y}_E)^T \cdot \mathbf{V}_E^{-1} \cdot (\mathbf{y}_k - \mathbf{y}_E)\right]\right\}, \qquad (2)$$

where $\mathbf{y}_E$ is the measured DDCSs, $\mathbf{V}_E$ is its associated covariance, and $\mathbf{y}_k$ is the DDCSs from the computer simulation k. In this framework, the covariance matrix is assumed to be diagonal. While this will lead to larger uncertainties in the results, it was chosen based on advice of the scientists who performed the experiment [8]. The experimental data were collected at the SEQUOIA detector at the SNS at incident energies 55, 160, 250, 600, 1,000, 3,000, and 5,000 meV between scattering angles of 3° and 58° with 1° increments. These weighting functions were then used to calculate the mean value of the dynamic structure factor, as well as its covariance,

$$\langle x_i \rangle = \lim_{K\to\infty} \frac{\sum_{k=1}^{K} x_{ik}\omega_k}{\sum_{k=1}^{K} \omega_k}, \qquad (3a)$$

$$\mathbf{V}_{i,j} = \lim_{K\to\infty} \frac{\sum_{k=1}^{K} x_{ik}x_{jk}\omega_k}{\sum_{k=1}^{K} \omega_k} - \langle x_i \rangle \langle x_j \rangle. \qquad (3b)$$

In this example, x_k represents the dynamic structure factor $S(q, E)$ of simulation k, and K is the total number of simulations. In this work, the covariance matrix was not calculated, as there would not be sufficient computational storage for the covariance matrix. Only the uncertainties were calculated, which is equivalent to calculating the diagonal of the covariance matrix.

RESULTS AND ANALYSIS

The mean dynamic structure factor and its uncertainty were used to calculate several different quantities. First, they were plotted against the DDCSs from the original SNS data, as shown in Fig. 1. In addition to the simulation and experimental data, the ENDF/B-VII.1 [9] and ENDF/B-VIII.β3 [10] results were plotted to show the differences that the simulation results has compared with them.

The green shaded area represents the simulation cross section ± 1 standard deviation away from the mean. These DDCSs were calculated by running the corresponding ACE files through the simplified MCNP input then applying the SNS resolution function to those results.

The plots are shown on a logarithmic y-axis to better show the entirety of the SNS data and its uncertainties. Based on these plots, the uncertainties seem to make a noticeable contribution to the DDCSs, straddling the values between the ENDF/B-VII.1 and ENDF/B-VIII.β3 results between 100-125 meV for the first plot and 175-225 meV for the second plot. The simulated results also appear to mostly be greater than the ENDF/B-VIII.β3 results, even when the ENDF/B-VIII.β3 results agree more favorably with the experimental data.

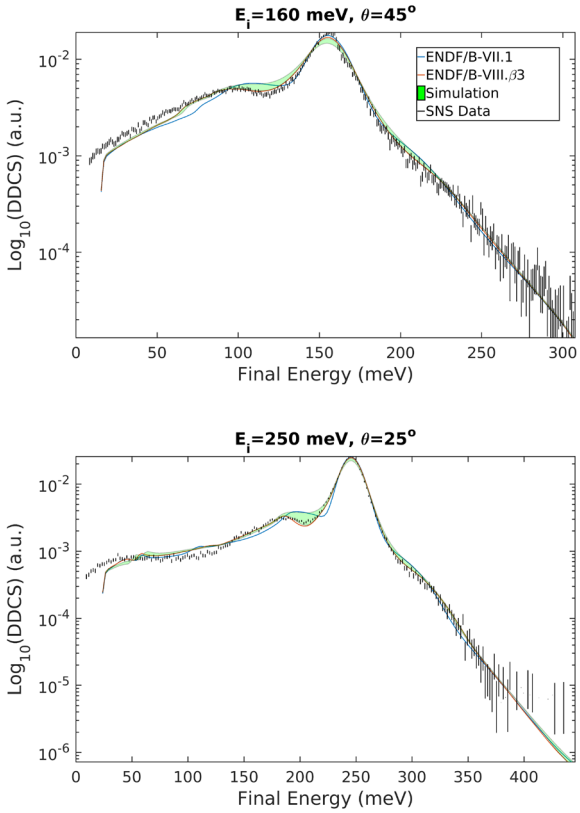

Fig. 1. Double differential scattering cross section for light water with incident energies and scattering angles 160 meV at 45° and 250 meV at 25°.

To further validate these results, additional DDCSs were plotted against independently gathered experimental data [11], shown in Fig. 2. The simulation results are from the same dynamic structure factor used to plot the DDCSs in Fig. 1. Because the exact experimental setup was not known for this set of data, the structure factor was plotted directly from the ENDF files as opposed to the previous set of DDCS plots. Experimental uncertainties are not shown because they were not reported by the original work. The significant difference in appearance between these plots and those shown in Fig. 1 can be attributed to the fact that these plots are on a linear y-axis, while the previous plots are shown on a logarithmic y-axis. Here, the simulation data appears to be comparable to both the ENDF/B-VII.1 and ENDF/B-VIII.β3 data.

In addition to the DDCSs, the total cross sections were calculated and plotted against several other experimentally gathered cross sections [12] [13] shown in Fig. 3. As before, the green band represents the simulation results ± 1 standard deviation. The simulation results seem be slightly less accurate than the ENDF/B-VIII.β3 results with regards to total cross section. This is similar to the phenomenon shown in Fig. 1. Even with this discrepancy, the simulated results agree very favorably with the experimental cross sections.

Finally, three different (ICSBEP) benchmarks were cho-

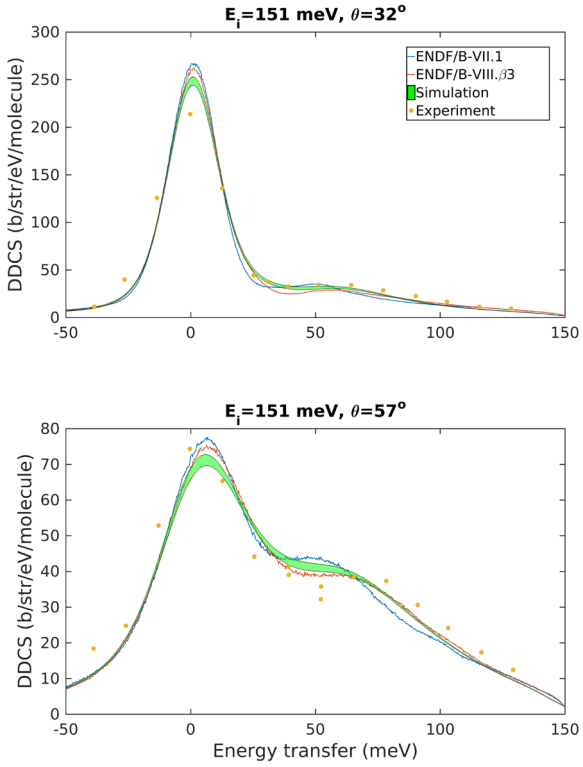

Fig. 2. Double differential scattering cross section for light water with incident energy 151 meV at scattering angles 32° and 57°. The cross sections are convoluted with the Gaussian resolution function with σ = 7.0 meV.

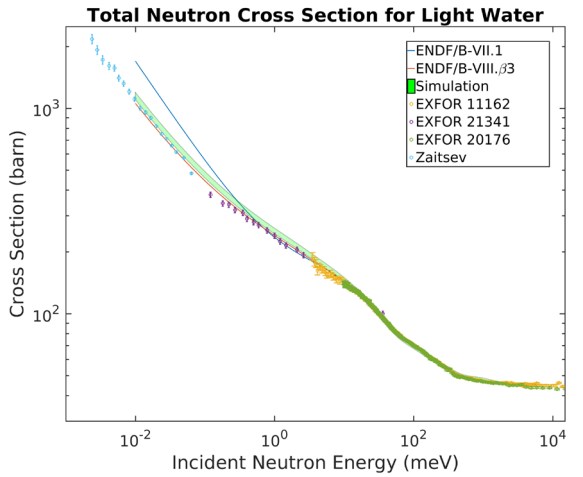

Fig. 3. Total neutron cross section for light water.

sen against which cross sections could be validated. The specific benchmarks (PST-033-003, LCT-079-007, and HCT-006-003) were chosen because they were all thermal systems and should have a difference in k_{eff} from varying the thermal scattering cross section of water. In addition to the mean value of the simulation results (New XS - Mean), the S(α,β) files were randomly perturbed according to their uncertainties, and 6 more simulations were run with those perturbed cross sections (New XS - Var. 1,2,...). This was done to establish a first-guess at the benchmark's sensitivity to thermal scattering.

XS library	k_{eff}	St.Dev (pcm)	Δk_{eff} (pcm)
Benchmark	1.00000	162	N/A
ENDF/B-VII.1	0.99349	4	651
ENDF/B-VIII.β3	0.99422	4	578
New XS - Mean	0.99483	4	517
New XS - Var. 1	0.99472	4	528
New XS - Var. 2	0.99471	4	529
New XS - Var. 3	0.99482	4	518
New XS - Var. 4	0.99473	4	527
New XS - Var. 5	0.99467	4	533
New XS - Var. 6	0.99493	4	507

TABLE I: Benchmark results for PST-033-003.

XS library	k_{eff}	St.Dev (pcm)	Δk_{eff} (pcm)
Benchmark	1.00030	80	N/A
ENDF/B-VII.1	0.99933	4	97
ENDF/B-VIII.β3	0.99982	4	48
New XS - Mean	1.00006	4	24
New XS - Var. 1	1.00000	4	30
New XS - Var. 2	0.99995	4	35
New XS - Var. 3	1.00026	4	4
New XS - Var. 4	1.00001	4	29
New XS - Var. 5	0.99961	4	69
New XS - Var. 6	1.00039	4	-9

TABLE II: Benchmark results for LCT-079-007.

XS library	k_{eff}	St.Dev (pcm)	Δk_{eff} (pcm)
Benchmark	0.97690	490	N/A
ENDF/B-VII.1	0.98190	4	-500
ENDF/B-VIII.β3	0.98232	4	-542
New XS - Mean	0.98245	4	-555
New XS - Var. 1	0.98235	4	-545
New XS - Var. 2	0.98222	4	-532
New XS - Var. 3	0.98269	4	-579
New XS - Var. 4	0.98225	4	-535
New XS - Var. 5	0.98187	4	-497
New XS - Var. 6	0.98290	4	-600

TABLE III: Benchmark results for HCT-006-003.

The results from the PST benchmark are shown in Table I. The benchmark shows that the simulation results get closer to the benchmark results, and they are not overly sensitive to thermal scattering, based on the change of eigenvalue between the maximum and minimum values (26 pcm). The difference

between the ENDF/B-VIII.β3 and simulation results is 61 pcm, which is a greater difference than the previously mentioned 26 pcm range of the 6 variations to the cross sections.

The LCT benchmark results in Table II also show that the simulation results get closer to the benchmark results, but the ENDF/B-VIII.β3 and simulation results both fall within the standard deviation of the benchmark uncertainty, so it is not as meaningful as with the PST benchmark. Even with an eigenvalue difference of 78 pcm between the maximum and minimum variations, the varied simulations fall within the uncertainty of the benchmark.

The HCT results in Table III show the simulation seems to do worse than the ENDF/B-VIII.β3 library at calculating the eigenvalue, and it is the most sensitive, exhibiting a difference of 103 pcm between the maximum and minimum variations. This specific benchmark has a very large uncertainty (490 pcm), and the ENDF/B-VIII.β3 and simulation results are both just outside this uncertainty threshold.

One interesting note about these benchmarks is that the simulation cross sections yielded a larger eigenvalue than either the ENDF/B-VII.1 or ENDF/B-VIII.β3. This is most likely due to the fact that the simulation cross section is greater than the both of them around the 1-10 meV range, as shown in Fig. 3. These benchmarks were originally chosen because they exhibited a negative sensitivity in the thermal energy range, but it appears that the overall increase in total cross section outweighs the negative sensitivity at the thermal range.

CONCLUSIONS AND FUTURE WORK

A framework for generating thermal scattering kernels and their covariances is presented. While only the uncertainties are calculated here, the capabilities to generate the covariance data are provided. The resulting DDCSs and total cross sections agree very favorably with both SNS and independent experimental data, in some cases better than the ENDF/B-VII.1 and ENDF/B-VIII.β3 data. It also resulted in definitive improvements in one of the three criticality benchmarks, as well as plausible improvement for the LCT benchmark. It would be beneficial to validate these cross sections against other benchmarks, preferably with smaller benchmark uncertainty in their eigenvalue results. While the framework outlines how to generate the covariance data, there is still no method to propagate thermal scattering covariance data through neutron transport codes. In addition, the framework can be applied to any material, and there is an interest in this application for other thermal materials for reactor and criticality safety applications, such as graphite, lucite, or teflon.

ACKNOWLEDGMENTS

The primary author would like to acknowledge the support provided by the U.S. Department of Energy Nuclear Energy University Program Graduate Fellowship. He would also like to thank Kemal Ramic and Carl Wendorff of RPI for their help in providing the data, as well as Garrett Granroth and Alexander Kolesnikov of the ORNL SNS for their assistance in providing the SNS resolution function. This research used resources of the National Energy Research Scientific Computing Center, a DOE Office of Science User Facility supported by the Office of Science of the U.S. Department of Energy under Contract No. DE-AC02-05CH11231. The work by Dr. Yaron Danon and Dr. Goran Arbanas was supported by the DOE Nuclear Criticality Safety Program, funded and managed by the National Nuclear Security Administration for DOE.

REFERENCES

1. R. CAPOTE and D. SMITH, "An Investigation of the Performance of the Unified Monte Carlo Method of Neutron Cross Section Data Evaluation," *Nuclear Data Sheets*, **109**, 2768–2773 (2008).
2. V. D. SPOEL ET AL., "GROMACS: Fast, flexible, and free," *Journal of Computational Chemistry*, **26**, 1701–1718 (2005).
3. M. GONZÁLEZ and J. ABASCAL, "A flexible model for water based on TIP4P/2005," *The Journal of Chemical Physics*, **26**, 224516 (2011).
4. Y. ABE and S. TASAKI, "Molecular dynamics analysis of incoherent neutron scattering from light water via the Van Hove space-time self-correlation function with a new quantum correction," *Annals of Nuclear Engineering*, **83**, 302–308 (2015).
5. L. VAN HOVE, "Correlations in Space and Time and Born Approximation Scattering in Systems of Interacting Particles," *Physical Review*, **95**, 249–262 (1954).
6. J. GOORLEY, M. JAMES, ET AL., "Initial MCNP6 Release Overview," Tech. Rep. LA-UR-13-22934, Los Alamos National Laboratory (2013).
7. R. MACFARLANE and D. MUIR, "The NJOY Nuclear Data Processing System," Tech. Rep. LA-12740-M, Los Alamos Scientific Laboratory (1994).
8. G. GRANROTH, private communication (2016).
9. M. CHADWICK ET AL., "ENDF/B-VII.1 Nuclear Data for Science and Technology: Cross Sections, Covariances, Fission Product Yields and Decay Data," *Nuclear Data Sheets*, **112**, 2887–2996 (2011).
10. J. MARQUEZ DAMIAN, D. MALASPINA, and J. GRANADA, "CAB models for water: A new evaluation of the thermal neutron scattering laws for light and heavy water in ENDF-6 format," *Annals of Nuclear Engineering*, **65**, 280–289 (2014).
11. O. HARLING, "Slow Neutron Inelastic Scattering Study of Light Water and Ice," *The Journal of Chemical Physics*, **50**, 5279–5296 (1969).
12. N. OTUKA, E. DUPONT, V. SEMKOVA, ET AL., "Towards a More Complete and Accurate Experimental Nuclear Reaction Data Library (EXFOR): International Collaboration Between Nuclear Reaction Data Centres (NRDC)," *Nuclear Data Sheets*, **120**, 272–276 (2014).
13. K. ZAITSEV, V. PETROV, S. KUZNETSOV, O. LANGER, I. MESHKOV, and A. PEREKRESTENKO, "The total cross sections of the interaction of ultracold neutrons with H_2O and D_2O," *Atomic Energy*, **70**, 238–242 (1991).